*Environ. Sci. Technol.* **1998**, *32,* 1994−2003

# Nitrogen Dioxide Absorption and Sulfite Oxidation in Aqueous Sulfite

CHEN H. SHEN AND GARY T. ROCHELLE*
*Department of Chemical Engineering, The University of Texas at Austin, Austin, Texas 78712-1062*

Removal of NO from flue gas may be achieved by its oxidation to $NO_2$ followed by absorption in sulfite solution in existing scrubbers for desulfurization. Rates of $NO_2$ absorption and sulfite oxidation were measured in a highly characterized stirred-cell contactor. The results were interpreted by the theory of mass transfer with fast reaction in the boundary layer. The reactions between $NO_2$ and sulfite ($SO_3^{2-}$), bisulfite ($HSO_3^-$), and thiosulfate ($S_2O_3^{2-}$) were first order in $NO_2$ concentration, and their respective rate constants at 55 °C were $11.2 \times 10^5$, $2.8 \times 10^4$, and $5.4 \times 10^3$ $M^{-1}$ $s^{-1}$. The $NO_2$ hydrolysis reaction was second order in $NO_2$ concentration, with a rate constant of $1.6 \times 10^7$ $M^{-1}$ $s^{-1}$ at 55 °C. $NO_2$ absorption initiates sulfite oxidation in the presence of oxygen, and this study quantified the effect of sulfite and oxygen concentration, the rate of $NO_2$ absorption, and the presence of thiosulfate and gas-phase $SO_2$ on the rate of sulfite oxidation. With typical conditions for limestone slurry, 10 mM total dissolved S(IV) and pH 4−5, the estimated $NO_2$ removal was less than 50%. Therefore, an acceptable level of $NO_2$ removal by a conventional limestone slurry scrubber is not probable. However, $NO_2$ absorption is feasible in sodium sulfite inhibited by thiosulfate. $NO_2$ may also be an effective catalyst for sulfite oxidation in limestone slurry scrubbing.

## Introduction

Limestone ($CaCO_3$) slurry scrubbing and lime (CaO) spray drying are state-of-the-art technologies for flue gas desulfurization. These systems do not remove NO because of its limited solubility and reactivity. However, $NO_2$ is reactive with sulfite solutions and will be removed to a significant extent by these systems. NO can be converted to $NO_2$ by the addition of methanol at >400 °C (*1*) or by the addition of ozone (*2, 3*) or hydrogen peroxide (*4*). Therefore, it may be feasible to achieve simultaneous $SO_2$ and $NO_x$ removal by the combination of NO oxidation and conventional scrubbing of $SO_2$. In a typical limestone slurry scrubbing operation, dissolved sulfite is oxidized to sulfate by sparging air into the slurry hold tank. Since $NO_2$ absorption is shown to initiate sulfite oxidation, another possible application is to reduce oxidation air stoichiometry or to reduce the depth of the hold tank by injecting small amounts of $NO_2$ into the oxidation air.

$NO_2$ absorption occurs with simultaneous mass transfer and fast reaction. Although previous investigators have studied $NO_2$ reaction with sulfite, these studies were usually performed under conditions far from that of a limestone slurry scrubber. Takeuchi et al. (*5*) measured $NO_2$ absorption into aqueous sodium sulfite and bisulfite solutions, both in a gas liquid contactor and a spray column, and they have reported the reaction rate constant for the above reaction at 25 °C. They have studied the effect of sulfite concentration, gas-phase $NO_2$ partial pressure, and agitation on the rate of $NO_2$ absorption. They have investigated the effect of temperature between 10 and 25 °C. In another study, Takeuchi et al. (*6*) performed simultaneous absorption of $SO_2$ and $NO_2$ in aqueous solutions of NaOH and $Na_2SO_3$. Pigford et al. (*7*) studied the absorption of $NO_2$ into water, sulfuric acid, NaOH, and alkaline $Na_2SO_3$ solutions in a wetted sphere absorber. Their results show that the dimer form of $NO_2$ ($N_2O_4$) is the actual species being absorbed, and they have proposed a reaction mechanism to account for this observation.

$NO_2$ reacts with sulfite through a free radical mechanism (*8*), with the net result being that every mole of $NO_2$ absorbed can lead to the oxidation of 4 or more moles of sulfite in the presence of oxygen. Furthermore, it has been shown that the rate of sulfite oxidation is strongly affected by the presence of $NO_2$, especially when $O_2$ is also present in the gas phase.

There are several different objectives for this study. First, it seeks to expand our understanding of the reaction mechanism by measuring and reporting kinetic rate constants at both 25 and 55 °C. Second, this study covered a much wider range of sulfite and $NO_2$ concentration than any previous researchers, in particular the additional presence of $SO_2$ and $O_2$ in the gas phase and thiosulfate in the solution. Third, it develops a model to account for sulfite oxidation in the presence of $NO_2$, supported by actual measurements of oxidation rates. Finally, this paper attempts to predict the performance of a typical limestone slurry scrubber in removing $NO_2$ and proposes other possible applications of our results.

## Experimental Method

All experiments were performed in a stirred cell contactor with separately agitated gas and liquid. The gas/liquid contact area was 81 $cm^2$. Details on the apparatus and experimental methods are same as those for $NO_2$ absorption in sulfide solutions (*9, 10*). This same reactor was used for $SO_2$ absorption in $Ca(OH)_2$ slurries (*11*).

The stirred-cell contactor was operated either continuously or in batch mode. When operating in the batch mode, the solution was fed into the reactor before each experiment and was withdrawn after each run. Nothing was added or withdrawn during the course of the experiment. While this mode of operation had the advantage of simplicity, the sulfite concentration in the solution as well as the solution pH was continuously decreasing during the course of a run, which was undesirable for most of our studies. Therefore, the majority of our experiments were performed with continuous operation.

When operating in a continuous mode, a solution containing $Na_2SO_3$, $Na_2SO_4$, and other additives such as succinic acid and sodium thiosulfate was freshly prepared and fed into the contactor. Succinic acid was added to a number of experiments to buffer the pH at the gas/liquid interface. Succinic acid is similar in buffer function to glutaric and adipic acids, common buffer additives for limestone slurry scrubbing. Sodium thiosulfate was used as an inhibitor of sulfite oxidation. The pH of the solution was adjusted by adding NaOH. Between 100 and 300 mM $Na_2SO_4$ was used to keep a constant ionic strength for all the runs. Once the run began, a mixture of $Na_2SO_3$/$NaHSO_3$/NaOH of predetermined concentration was periodically fed into the contactor for the purpose of maintaining a constant solution pH

* Address correspondence to this author. Fax: (512)471-7060; e-mail: rochelle@che.utexas.edu.


S0013-936X(97)00466-5 CCC: $15.00 © 1998 American Chemical Society
Published on Web 05/27/1998

and total S(IV) concentration, and the same volume of solution was withdrawn from the contactor at the same time for solution analysis. Important variables such as the pressure inside the contactor, the temperature, the solution pH, and the liquid and gas agitation rates were monitored and controlled.

The rates of sulfite oxidation and oxygen absorption were determined by iodimetric titration of the samples to get total S(IV) and thiosulfate in the solution. When only $SO_3^{2-}/HSO_3^-$ was present, the concentration of total S(IV) was determined by a one-step titration (*12*). An excess amount of iodine of known concentration was introduced into the sample, and then the sample was back-titrated with a standard thiosulfate solution until the color disappeared. When both $SO_3^{2-}$ and $S_2O_3^{2-}$ were present, the concentration of individual S(IV) and $S_2O_3^{2-}$ was determined by iodometric titration with and without formaldehyde (*13*). This procedure tracks only disappearance of S(IV) and assumes that oxidants and other interfering species such as $HSO_5^-$ are present at concentrations much less than the S(IV).

## Chemistry and Theory

The actual mechanism of the reaction between $NO_2$ and aqueous sulfite solution is rather complex. Nash (*14*) proposed that such a reaction was likely to involve charge transfer that might lead to a free radical chain mechanism. Three irreversible parallel reactions may occur in the boundary layer and enhance $NO_2$ absorption. These reactions are as follows:

$$NO_2 + SO_3^{2-} \rightarrow NO_2^- + SO_3^{\bullet -}$$
$$r_{SO_3^{2-}} = k_{2,SO_3^{2-}}[SO_3^{2-}]_i[NO_2]_i \quad (1)$$

$$NO_2 + HSO_3^- \rightarrow NO_2^- + HSO_3^{\bullet}$$
$$r_{HSO_3^-} = k_{2,HSO_3^-}[HSO_3^-]_i[NO_2]_i \quad (2)$$

$$2NO_2 + H_2O \rightarrow HNO_2 + HNO_3$$
$$r_{H_2O} = k_{2,H_2O}[NO_2]_i^2 \quad (3)$$

where $[SO_3^{2-}]_i$, $[HSO_3^-]_i$, and $[NO_2]_i$ are the interfacial concentrations of sulfite, bisulfite, and $NO_2$, respectively.

When thiosulfate is added to the solution, it can also react with $NO_2$ by the following reaction:

$$NO_2 + S_2O_3^{2-} \rightarrow NO_2^- + S_2O_3^{\bullet -}$$
$$r_{S_2O_3^{2-}} = k_{2,S_2O_3^{2-}}[S_2O_3^{2-}]_i[NO_2]_i \quad (4)$$

When $SO_2$ is added to the gas phase, the following equilibrium reaction takes place:

$$SO_2 + SO_3^{2-} + H_2O \leftrightarrow 2HSO_3^- \quad (5)$$

which has the net effect of increasing the concentration of total S(IV) in the solution while reducing the solution pH.

When absorbing $NO_2$ into sulfite solutions, assuming fast reactions and using the reaction kinetics at the gas/liquid interface, the flux of $NO_2$ ($N_{NO_2}$) should be given approximately by (*15, 16*)

$$N_{NO_2} = \frac{P_{NO_{2,i}}}{H_{NO_2}}\left[D_{NO_2}\left(k_{2,SO_3^{2-}}[SO_3^{2-}]_i + k_{2,HSO_3^-}[HSO_3^-]_i + \frac{2}{3}\frac{k_{2,H_2O}P_{NO_{2,i}}}{H_{NO_2}} + k_{2,S_2O_3^{2-}}[S_2O_3^{2-}]_i\right)\right]^{1/2} \quad (6)$$

Rearranging eq 6 to a linear form gives

$$\frac{R_g^2 H_{NO_2}^2}{D_{NO_2}} = k_{2,SO_3^{2-}}[SO_3^{2-}]_i + k_{2,HSO_3^-}[HSO_3^-]_i + \frac{2}{3}\frac{k_{2,H_2O}P_{NO_{2,i}}}{H_{NO_2}} + k_{2,S_2O_3^{2-}}[S_2O_3^{2-}]_i \quad (7)$$

where $R_g$ is a normalized rate of absorption given by the following:

$$R_g = \frac{N_{NO_2}}{P_{NO_{2,i}}} \quad (8)$$

$P_{NO2i}$ is the interfacial partial pressure of $NO_2$ and is given by

$$P_{NO_{2,i}} = P_{NO_{2,b}} - \frac{N_{NO_2}}{k_g} \quad (9)$$

where $P_{NO_{2,b}}$ is the measured bulk partial pressure of $NO_2$, and $k_g$ is the gas-phase mass transfer coefficient, measured by $SO_2$ absorption in NaOH solution (*9*):

$$k_g A\ [\text{mol s}^{-1}\ \text{bar}^{-1}] = 4.95 \times 10^{-5}\ (\text{gas agitation speed})^{0.76} \quad (10)$$

At 650 rpm, $k_g = 1.0 \times 10^{-4}$ mol cm$^{-2}$ s$^{-1}$ atm$^{-1}$. In the absence of gas film resistance, $R_g$ is identical to $K_g$, the overall gas-phase mass transfer coefficient. The diffusion coefficient of dissolved $NO_2$ ($D_{NO_2}$) was taken to be $3.28 \times 10^{-5}$ cm$^2$ s$^{-1}$ at 55 °C (*17*). The Henry's constant for $NO_2$ ($H_{NO_2}$) was taken to be $4.76 \times 10^4$ cm$^{-3}$ atm$^{-1}$ mol$^{-1}$ at 55 °C (*18*).

Oblath et al. (*19, 20*) studied the reactions between $NO_2$ and sulfite, and they found that the product of this reaction was a family of nitrososulfonates, including $HON(SO_3)_2^{2-}$, $HONHSO_3^-$, $HN(SO_3)_2^{2-}$, and $N(SO_3)_2^{2-}$. They found that the rates of these reactions are too small for them to occur to any significant extent in the boundary layer, so the formation of these nitrogen−sulfur compounds is expected to occur in the bulk solution.

In the presence of oxygen, the free radicals produced by $NO_2$ reaction with sulfite and bisulfite were found to initiate sulfite oxidation in a chain mechanism (*8, 21*). These reactions are expected to occur in the mass transfer boundary layer. One direct consequence of this mechanism is the depletion of sulfite in the liquid boundary. For every mole of $NO_2$ absorbed, several moles of $SO_3^{2-}$ can be consumed if oxygen is present. Therefore, when oxygen is present, the rate of $NO_2$ absorption is expected to be lower. Takeuchi et al. (*22*) observed that the absorption rate of $NO_2$ into sodium sulfite solution was about 40% lower in air rather than nitrogen. We believe that this difference was caused by the oxidation of sulfite by dissolved oxygen, and we have quantified this effect by accounting for sulfite depetion at the gas/liquid interface. The effect could also be caused by regeneration of $NO_2$ from nitrite in the presence of oxygen, but our results did not require this additional mechanism.

Owens (*23*) studied sulfite oxidation and thiosulfate degradation in FGD systems. He concluded that thiosulfate ($S_2O_3^{2-}$) was a strong inhibitor of sulfite oxidation. He suggested that thiosulfate could act as a free radical scavenger and thus was able to terminate the sulfite oxidation mechanism. In a system where $NO_2$ was absorbed into a sulfite

solution, thiosulfate could reduce the rate of sulfite oxidation by providing an alternative route for free radical termination:

$$R^{\bullet} + S_2O_3^{2-} \rightarrow R + S_2O_3^{\bullet -} \quad (11)$$

$$S_2O_3^{\bullet -} + S_2O_3^{\bullet -} \rightarrow S_4O_6^{2-} \quad (12)$$

The rate of sulfite oxidation ($N_{ox}$, mol cm$^{-2}$ s$^{-1}$) was calculated from experimental data with the following material balance:

$$N_{ox} = \frac{V([S(IV)]_o - [S(IV)]_f) + V_{tit}[S(IV)]_{tit}}{A\Delta t} + N_{SO_2} \quad (13)$$

where $[S(IV)]_o$ and $[S(IV)]_f$ are the initial and final concentration of total S(IV) measured by iodimetric titration, respectively; $\Delta t$ is the time interval; and $V$ and $A$ are the volume of the solution and the gas−liquid contacting area, respectively. The $V_{tit}[S(IV)]_{tit}$ term takes into account the amount of S(IV) being fed into the contactor over the course of one experiment, while the last term accounts for the additional sulfite formed by the absorption of $SO_2$.

To regress the four reaction rate constants from eq 7, it is necessary to have accurate estimates of $[SO_3^{2-}]_i$, $[HSO_3^-]_i$, and $[NO_2]_i$, the interfacial concentrations of sulfite, bisulfite, and $NO_2$. This was done by using the Bechtel-Modified Radian Equilibrium Program (BMREP) (*24*), an equilibrium program capable of calculating the concentrations of all major species in the $SO_3^{2-}$ system, given the ionic strength, pH, total [S(IV)] and [S(VI)], total $[Na^+]$ and other metal ions present, and the concentration of buffer. To calculate $[SO_3^{2-}]_i$ and $[HSO_3^-]_i$, the bulk solution $[SO_3^{2-}]$ and $[HSO_3^-]$ were first calculated by the equilibrium program, and then by using the experimentally measured rate of sulfite oxidation calculated in eq 13, the [S(IV)] at the interface was estimated from the following equation:

$$[S(IV)]_i = [S(IV)]_b - \frac{N_{ox}}{k_l^{\circ}{}_{S(IV)}} \quad (14)$$

This relationship assumes that all of the sulfite oxidation occurs near the gas/liquid interface. The equilibrium program was used again at interfacial condition to obtain the interfacial concentrations of sulfite and bisulfite. In the above equation, $k_l^{\circ}{}_{S(IV)}$ is the liquid-phase mass transfer coefficient of S(IV) species, which is taken to be the same as $k_l^{\circ}{}_{SO_3^{2-}}$. The liquid film mass transfer coefficient was measured by absorption of $SO_2$ in HCl solution (*9*). The value of $k_l^{\circ}{}_{SO_3^{2-}}$ is given as a function of liquid agitation:

$$k_l^{\circ}{}_{SO_3^{2-}}\,[m/s] = 6.13 \times 10^{-7}(\text{liquid agitation speed})^{0.65} \quad (15)$$

A parameter estimation program was then used to regress the four rate constants in the linear form of eq 7 for any given set of experiments.

## Results and Discussion

**Results of Continuous Experiments.** *$NO_2$ Absorption.* The results of the continuous experiments are given in Tables 1 and 2. Table 1 summarizes the results of continuous experiments in the absence of additives, while Table 2 gives the results with various liquid- and gas-phase additives. A series of experiments with 15% $O_2$ were regressed to obtain the rate constants from eq 7. We did not include experiments without oxygen, without buffer, with $SO_2$, or with other unusual conditions or poor data quality. Table 3 compares the regressed values of rate constants at 55 °C with those measured by Takeuchi at 25 °C. Table 4 gives selected results with other salts and additives.

Clifton et al. (*25*) report measured values of $k_{2,SO_3^{2-}}$ an order of magnitude larger ($1.2-2.9 \times 10^7$ M$^{-1}$ s$^{-1}$ at pH 5.3−13 and ambient temperature) than extracted from our absorption experiments. Furthermore, their rates did not decrease with pH as much as observed in our stirred-cell contactor. Their experiments were performed by pulsed radiolysis in the presence of 10 mM nitrite, 0.5−2 mM sulfite, and 5 $\mu$M $NO_2$. The time scale of Clifton's kinetic measurements was $10^{-4}$ s, as compared to 1 s in the stirred-cell contactor. The discrepancy in apparent rates suggests that the reaction mechanism may be more complicated than the simple mechanism successfully used to model the stirred cell results. It is possible that Clifton was measuring the formation of an addition complex such as $O_2NOSO_2^{2-}$. If such a complex were formed quickly and reversibly at an equilibrium concentration less than 10 times the $NO_2$ concentration, it would not affect the interpretation of the absorption results. The one detailed experiment reported by Clifton shows an exponential decay of $NO_2$ absorbance to a value significantly above the baseline, suggesting that their reaction with sulfite approaches an equilibrium conversion of about 90% in less than $10^{-4}$ s.

The relatively large confidence interval for $k_{2,H_2O}$ is due to the small number of pure water absorption experiments as well as the relatively minor contribution of the water reaction to the overall rate of $NO_2$ absorption in most of the experiments. However, the use of the full model in eq 7 is justified, since in most of the experiments, the reaction between $NO_2$ and $HSO_3^-$ and $S_2O_3^{2-}$ contributed significantly to the overall rate of $NO_2$ absorption.

The model predicts the effects of $O_2$, thiosulfate, and $SO_2$ on the rate of $NO_2$ absorption. In Tables 1 and 2, we used these fitted rate constants to calculate a rate of absorption for all the other experiments in Tables 1 and 2. The comparison is given as the ratio of the estimated and measured values of the normalized flux, $R_g$. All of the data fall within 10−30% of the model.

When $O_2$ is present in the gas phase, sulfite oxidation is enhanced, and the result is lower $SO_3^{2-}$ at the gas/liquid interface. Once this lower $[SO_3^{2-}]_i$ is accounted for by the model, these data points are represented quite well.

The effect of $SO_2$ depends on the buffer concentration. For every mole of $SO_2$ absorbed, 1 mol of $SO_3^{2-}$ is consumed, and 2 mol of $HSO_3^-$ is formed. The net effect of $SO_2$ absorption is an increase in total S(IV) concentration and a drop in pH at the interface. When a buffer such as succinate is present in the liquid phase, the change in pH is minimized, and the absorption of $SO_2$ leads to an increase in the rate of $NO_2$ absorption by adding to the total amount of S(IV). On the other hand, when no buffer is present, $SO_2$ absorption tends to inhibit the rate of $NO_2$ absorption by reducing the pH at the liquid boundary and reducing the fraction of S(IV) present as sulfite.

Figure 1 gives the normalized rate of $NO_2$ absorption ($R_g$) calculated by eq 7 as a function of pH and dissolved S(IV). The rate of $NO_2$ absorption increases with increasing S(IV) and pH, as both conditions lead to higher concentrations of $SO_3^{2-}$ in the solution. Because the experimental data points include ranges of S(IV), they do not fall on the calculated lines at exact values of S(IV).

Table 4 gives selected results with significant concentrations of major ions expected in limestone slurry scrubbing. The rates of $NO_2$ absorption and sulfite disappearance were estimated from eq 6. Equation 6 overpredicts $NO_2$ absorption rates in the experiments with 600 mM chloride ($Na^+$, $Ca^{2+}$, and $Mg^{2+}$) by 60%. It is possible that the dichloride radical

**TABLE 1. Summary of Continuous Results, No Additive, 55 °C**

| pH | $[S(IV)]_b$ (mM) | $[SO_3^{2-}]_b$ (mM) | $[SO_3^{2-}]_i$ (mM) | $P_{NO_2,i} \times 10^6$ (atm) | $O_2$ (%) | $R_{g,exp} \times 10^6$ (mol/(cm$^2$ s atm)) | $R_{g,mod}/R_{g,exp}$ [c] | $N_{ox} \times 10^8$ (mol/(cm$^2$ s)) | $N_{ox,mod}/N_{ox,exp}$ [d] | $Na_2SO_4$ (M) | succinate (M) |
|---|---|---|---|---|---|---|---|---|---|---|---|
| 4.5 | 40.9 | 0.63 | 0.54 | 79.8 | 15 | 4.8[a] | 1.02 | 2.31[b] | 0.86 | 0.25 | 0.1 |
| 5.0 | 0 | 0 | 0 | 106 | 15 | 0.98[a] | 1.01 | | | 0.3 | 0.1 |
| 5.0 | 0 | 0 | 0 | 129 | 15 | 1.1[a] | 1.10 | | | 0.3 | 0.1 |
| 5.0 | 6.77 | 0.32 | 0.26 | 92 | 15 | 2.7[a] | 0.99 | 0.49[b] | 0.92 | 0.29 | 0.1 |
| 5.0 | 7.41 | 0.16 | 0 | 136 | 15 | 2.5[a] | 0.97 | 0.30[b] | 1.02 | 0.29 | 0.3 |
| 5.0 | 38.0 | 2.0 | 1.56 | 65 | 15 | 6.1[a] | 0.98 | 3.47[b] | 1.11 | 0.25 | 0.3 |
| 5.0 | 38.8 | 1.5 | 1.2 | 94 | 15 | 5.1[a] | 0.98 | 2.97[b] | 0.95 | 0.25 | 0.1 |
| 5.0 | 39.6 | 1.49 | 1.38 | 80 | 15 | 3.1[a] | 1.03 | 2.74[b] | 1.05 | 0.25 | 0.3 |
| 5.1 | 1.43 | 0.036 | 0 | 136 | 15 | 2.5[a] | 0.98 | 0.30 | | 0.3 | 0.1 |
| 5.5 | 14.8 | 0.98 | 0.63 | 156 | 15 | 3.9[a] | 0.99 | 1.23[b] | 0.75 | 0.29 | 0.1 |
| 6.0 | 73.4 | 14.9 | 2.88 | 172 | 15 | 15.2[a] | 1.00 | 2.96 | 0.10 | 0.2 | 0.1 |
| 4.5 | 42.5 | 0.64 | 0.56 | 82.4 | 0 | 4.4 | 0.95 | 0.26 | | 0.25 | 0.1 |
| 5.0 | 16.2 | 0.34 | 0.27 | 216 | 0 | 2.7 | 1.12 | 0.28 | | 0.29 | 0.1 |
| 5.0 | 42.2 | 1.9 | 1.61 | 88 | 0 | 6.1 | 0.81 | 0.25 | | 0.25 | 0.1 |
| 5.1 | 1.74 | 0.045 | 0 | 133 | 0 | 2.8 | 1.09 | 0.27 | | 0.3 | 0.1 |
| 5.0 | 13.2 | 0.27 | 0.11 | 227 | 0 | 2.2 | 0.98 | 0.30 | | 0.09 | |
| 5.1 | 45.3 | 2.5 | 1.08 | 79 | 0 | 6.3 | 2.06 | 0.24 | | 0.25 | |
| 5.5 | 10 | 0.68 | 0.29 | 80 | 0 | 5.3 | 0.74 | 0.24 | | 0.096 | |
| 5.0 | 0 | 0 | 0 | 131 | 15 | 0.89 | 0.82 | | | | |
| 5.0[e] | 10 | 0.2 | 0 | 38 | 15 | 1.0 | 0.68 | 0.60 | 0.72 | 0.096 | |
| 5.0[e] | 10 | 0.22 | 0 | 290 | 15 | 2.2 | 0.75 | 0.73 | | 0.096 | |
| 5.0[e] | 10 | 0.35 | 0 | 42 | 15 | 0.9 | 0.61 | 0.53 | 0.58 | 0.096 | |
| 5.1 | 43.4 | 2.1 | 0.32 | 85 | 15 | 5.3 | 1.28 | 3.22[b] | 1.15 | 0.25 | |
| 5.4 | 10.8 | 0.9 | 0 | 500 | 15 | 3.3 | 1.64 | 0.94 | | 0.096 | |
| 5.5 | 10 | 0.54 | 0 | 75 | 15 | 2.0 | 0.61 | 0.98 | 0.45 | 0.096 | |
| 5.5 | 10 | 0.63 | 0 | 97 | 15 | 1.9 | 0.68 | 1.82[b] | 1.08 | 0.096 | |
| 5.5 | 10 | 0.59 | 0 | 105 | 15 | 1.6 | 0.52 | 1.30 | 0.77 | 0.096 | |
| 5.5 | 10 | 0.68 | 0 | 116 | 15 | 1.3 | 0.59 | 0.66 | | 0.096 | |
| 6.0 | 10 | 1.8 | 0.16 | 65 | 15 | 4.3 | 1.53 | 1.02 | 0.10 | 0.096 | |
| 6.0[f] | 87.0 | 17.5 | 3.2 | 15 | 15 | 15.4 | 1.24 | 4.76 | 1.28 | 0.2 | |
| 6.0[f] | 87.0 | 14.5 | 0.73 | 233 | 15 | 12.3 | 0.79 | 8.20 | 1.22 | 0.2 | |
| 6.0[f] | 87.0 | 14.0 | 0.65 | 16 | 15 | 18.1 | 0.85 | 10.8 | 1.78 | 0.2 | |
| 4.9 | 8.32 | 0.31 | 0.14 | 85 | 15 | 7.5 | 0.39 | 0.68 | | 0.29 | 0.1 |
| 5.7 | 6.76 | 1.304 | 1.05 | 58 | 15 | 2.1 | 1.35 | 0.62[b] | 1.12 | 0.25 | 0.1 |
| 5.58 | 6.96 | 1.087 | 0.66 | 53.3 | 15 | 2.63 | 1.31 | 0.50 | | 0.25 | 0.1 |
| 5.58 | 6.77 | 1.023 | 0.84 | 52.2 | 5 | 3.06 | 1.13 | 3.21 | 1.51 | 0.25 | 0.1 |
| 5.64 | 6.68 | 0.963 | 0.82 | 35.3 | 1 | 3.53 | 1.20 | 15.1[b] | 0.99 | 0.25 | 0.1 |
| 5.52 | 7.73 | 1.016 | 0.78 | 45.8 | 10 | 5.21 | 0.85 | 2.00[b] | 0.92 | 0.25 | 0.1 |
| 5.38 | 80.7 | 9.408 | 8.32 | 52.1 | 15 | 9.72 | 1.18 | 5.96[b] | 1.06 | 0.20 | 0.2 |
| 5.46 | 46.8 | 6.55 | 5.74 | 69.1 | 15 | 4.70 | 1.86 | 4.16 | 0.87 | 0.25 | 0.15 |
| 5.48 | 9.887 | 1.29 | 1.04 | 245.1 | 15 | 3.43 | 1.28 | 1.91 | 0.09 | 0.25 | 0.1 |
| 5.52 | 42.22 | 6.456 | 4.82 | 350.2 | 15 | 7.28 | 1.21 | 7.43 | 1.30 | 0.25 | 0.15 |

[a] These runs were used to regress the reaction rate constants $k_{2,SO_3^{2-}}$, $k_{2,HSO_3^-}$, $k_{2,H_2O}$, and $k_{2,S_2O_3^{2-}}$ from eq 7. [b] These runs were used to regress the oxidation rate constants $C_1$ and $C_2$ from eq 16. [c] The ratio of values of the normalized $NO_2$ flux ($R_g$) calculated from eq 6 and measured values. [d] The ratio of values of the oxidation flux ($N_{ox}$) calculated from eq 16 to measured values. [e] N products were allowed to accumulate to 0.2 mM in the second and third run of this series. [f] N products were allowed to accumulate to 1.3 mM in the second and third run of this series.

participates in the mechanism to regenerate $NO_2$ and slow the net rate of $NO_2$ absorption.

The results with 500 mM $MgSO_4$ suggest that there is no significant effect of the cation on $NO_2$ absorption. The model calculation accounts for the complexing effect of $Mg^{2+}$ by assuming that sulfite ion pairs with $Ca^{2+}$ and $Mg^{2+}$ are unreactive to $NO_2$. Previous work by Takeuchi et al. (*5*) showed that rates of $NO_2$ absorption in 0.1 M $Na^+$, $K^+$, and $NH_4^+$ varied by less than 20%. The experiments with added EDTA and $Fe^{2+}$ had no significant effects on $NO_2$ absorption.

Most of the experiments reported here did not run long enough to permit the accumulation of products from sulfite oxidation or $NO_2$ absorption at levels that could affect the measured rates. However, in two series of experiments reported in Table 1, nitrogen products were allowed to accumulate to 0.2 and 1.3 mM (pH 5 and pH 6), respectively, by absorbing a high concentration of $NO_2$ for an extended period of time. The absorption rate of $NO_2$ was practically unaffected by the accumulation of nitrogen reaction products. The sulfite oxidation rate was unchanged at pH 5 but increased a factor of 2 at pH 6. In both series, analysis of the solutions by ion chromatography recovered practically all of the absorbed $NO_2$ as 21% hydroxylamine disulfonic acid, 62% amine disulfonic acid, 12% nitrate, and 5% nitrite.

*Sulfite Oxidation.* We found that the rate of sulfite oxidation was strongly influenced by the presence of $NO_2$, and there is a direct correlation between the rate of sulfite oxidation and the rate of $NO_2$ absorption. To quantify this effect of $NO_2$ absorption on sulfite oxidation, we developed a semiempirical correlation of sulfite oxidation:

$$N_{ox} = C_1\sqrt{N_{NO_2}}[O_2]_i + C_2\sqrt{N_{NO_2}}[SO_3^{2-}]_i + k_l^\circ{}_{O_2}[O_2]_i \quad (16)$$

The first term accounts for sulfite oxidation limited by $O_2$ in the liquid phase, the second term accounts for oxidation limited by $SO_3^{2-}$, and the last term accounts for physical absorption of oxygen. The liquid-phase mass transfer coefficient of $O_2$, $k_l^\circ{}_{O_2}$, was calculated from eq 15. The diffusivity of dissolved $O_2$ ($D_{O_2}$) was taken to be $4.79 \times 10^{-5}$ cm$^2$ s$^{-1}$ at 55 °C. The Henry's constant for oxygen was taken to be 60 850 atm/mol fraction from Perry's Handbook. A series of experiments was chosen from Tables 1 and 2, and a parameter estimation program was used to estimate the constants $C_1$ and $C_2$. We did not include experiments without

**TABLE 2. Summary of Continuous Results, with Additives, 55 °C**

| pH | $[S(IV)]_b$ (mM) | $[SO_3^{2-}]_b$ (mM) | $[SO_3^{2-}]_i$ (mM) | $P_{NO_2,i} \times 10^6$ (atm) | $O_2$ (%) | $R_{g,exp} \times 10^6$ (mol/(cm² s atm)) | $R_{g,mod}/R_{g,exp}$ [c] | $N_{ox} \times 10^8$ (mol/(cm² s)) | $N_{ox,mod}/N_{ox,exp}$ [d] | $Na_2SO_4$ (M) | additive | succinate (M) |
|---|---|---|---|---|---|---|---|---|---|---|---|---|
| 5.51 | 12.5 | | 1.94 | 86.1 | 0 | 10.3 | 0.88 | | | 0.25 | 35.9 ppm $SO_2$ | 0.1 |
| 5.52 | 14.8 | | 2.28 | 60.1 | 0 | 8.48 | 0.90 | | | 0.25 | 36.8 ppm $SO_2$ | 0.1 |
| 5.51 | 16.3 | | 2.33 | 42.8 | 0 | 8.41 | 0.93 | | | 0.25 | 24.5 ppm $SO_2$ | 0.1 |
| 5.51 | 11.9 | | 1.65 | 45.4 | 15 | 3.28 | 0.95 | 1.63 | 0.90 | 0.25 | 25.3 ppm $SO_2$ | 0.1 |
| 5.51 | 12.5 | | 1.58 | 56.1 | 15 | 2.10 | 0.99 | 1.86 | 0.85 | 0.25 | 16.7 ppm $SO_2$ | 0.1 |
| 5.46 | 0.97 | | 1.45 | 228.5 | 0 | 2.30 | 1.18 | | | 0.25 | 105.8 ppm $SO_2$ | 0.1 |
| 5.48 | 2.37 | | 1.35 | 230.1 | 15 | 2.23 | 1.23 | 0.63 | 1.11 | 0.25 | 106.8 ppm $SO_2$ | 0.1 |
| 4.45 | 12.4 | 0.9 | 0.81 | 242 | 15 | 2.18 | 1.13 | 1.93 | 1.07 | 0.25 | 117 ppm $SO_2$ | 0.1 |
| 4.48 | 17.0 | 0.38 | 0.23 | 248 | 15 | 3.10 | 0.92 | 2.93 | 0.81 | 0.25 | 111 ppm $SO_2$ | 0.1 |
| 9.87 | 72.1 | 78.9 | 54.0 | 168 | 15 | 9.2 | 1.22 | 14.5 | 1.05 | 0.15 | | |
| 9.78 | 78.9 | 78.9 | 57.9 | 96 | 15 | 19.0 | 1.02 | 11.8 | 1.21 | 0.15 | 68 ppm $SO_2$ | |
| 9.96 | 76.8 | 76.8 | 70.5 | 24 | 15 | 19.3 | 1.15 | 9.63 | 1.13 | 0.2 | | |
| 9.91 | 81.1 | 81.1 | 75.2 | 34 | 15 | 20.0 | 1.14 | 11.6 | 1.24 | 0.2 | | |
| 5.53 | 89.3 | | 14.2 | 47.3 | 0 | 11.3 | 1.15 | | | | 90 mM $S_2O_3^{2-}$ | |
| 5.57 | 81.5 | | 13.8 | 49.9 | 15 | 10.3[a] | 1.27 | 0.41[e] | 1.18 | | 90 mM $S_2O_3^{2-}$ | |
| 5.4 | 91 | | 9.8 | 46.1 | 0 | 9.11 | 1.20 | | | | 7.0 mM $S_2O_3^{2-}$ | |
| 5.4 | 82.9 | | 8.5 | 46.3 | 15 | 9.15[a] | 1.12 | 0.53[e] | 1.34 | | 7.0 mM $S_2O_3^{2-}$ | |
| 5.63[b] | 0 | 0 | 0 | 91.2 | 0 | 2.31 | | | | | 88.7 mM $S_2O_3^{2-}$ | |
| 5.46[b] | 0 | 0 | 0 | 90.3 | 15 | 2.41 | | | | | 87 mM $S_2O_3^{2-}$ | |
| 5.83 | 0 | 0 | 0 | 98.1 | 0 | 1.88 | 0.86 | | | | 86.1 mM $S_2O_3^{2-}$ | |
| 6.03 | 0 | 0 | 0 | 90.6 | 15 | 2.66[a] | 0.91 | | | | 88.4 mM $S_2O_3^{2-}$ | |
| 6.11[b] | 86.0 | | 33.3 | 63.1 | 0 | 7.67 | | | | | 8.2 mM $S_2O_3^{2-}$ | |
| 6.14[b] | 79.4 | | 31.8 | 68.7 | 15 | 6.42 | | 0.37 | | | 6.7 mM $S_2O_3^{2-}$ | |
| 7.71 | 98 | 93 | 85.8 | 17.2 | 15 | 36[a] | 0.83 | 3.19[e] | 0.81 | | 103 mM $S_2O_3^{2-}$ | |
| 7.70 | 84 | 80 | 74.5 | 150.7 | 15 | 24[a] | 1.05 | 2.86[e] | 1.21 | | 99.2 mM $S_2O_3^{2-}$ | |
| 7.45 | 103 | 91 | 82.5 | 21.0 | 15 | 33[a] | 0.90 | 3.52[e] | 1.28 | | 10.2 mM $S_2O_3^{2-}$ | |
| 7.35 | 81 | 70 | 60 | 185.7 | 15 | 19[a] | 1.14 | 4.10[e] | 0.95 | | 9.2 mM $S_2O_3^{2-}$ | |
| 7.65 | 9.9 | 8.5 | 7.5 | 15.2 | 15 | 10[a] | 0.90 | 0.43[e] | 1.00 | | 10.3 mM $S_2O_3^{2-}$ | |
| 7.49 | 6.2 | 5.1 | 3.3 | 190.1 | 15 | 4.3[a] | 1.12 | 0.81[e] | 0.86 | | 9.5 mM $S_2O_3^{2-}$ | |
| 7.81 | 10.7 | 10.0 | 9.6 | 17.5 | 15 | 12[a] | 0.84 | 0.32[e] | 0.78 | | 103 mM $S_2O_3^{2-}$ | |
| 7.86 | 8.6 | 8.1 | 7.7 | 177.1 | 15 | 6.1[a] | 1.24 | 0.46[e] | 1.03 | | 104 mM $S_2O_3^{2-}$ | |

[a] These runs were used to regress the reaction rate constants $k_{2,SO_3^{2-}}$, $k_{2,HSO_3^-}$, $k_{2,H_2O}$, and $k_{2,S_2O_3^{2-}}$ from eq 7. [b] $T = 25$ °C. Our model of $NO_2$ absorption and sulfite oxidation do not apply to these runs. [c] The ratio of values of the normalized $NO_2$ flux ($R_g$) calculated from eq 6 to measured values. [d] The ratio of values of the oxidation flux ($N_{ox}$) calculated from eq 16 (or eq 22 with thiosulfate) to measured values. [e] These runs were used to regress the ratio $k_{ox}/k_t$ from eq 22, and $N_{ox}$ is calculated using eq 22.

**TABLE 3. Regressed Values of Rate Constants**

| reaction | reaction rate constant ($M^{-1} s^{-1}$) regressed at 55 °C | Takeuchi (*5*) at 25 °C |
|---|---|---|
| $k_{2,SO_3^{2-}}$ | $(11.2 \pm 0.3) \times 10^5$ | $6.6 \times 10^5$ |
| $k_{2,HSO_3^-}$ | $(2.8 \pm 0.1) \times 10^4$ | $1.5 \times 10^4$ |
| $k_{2,H_2O}$ | $(1.6 \pm 1.1) \times 10^7$ | $7.4 \times 10^7$ |
| $k_{2,S_2O_3^{2-}}$ | $(5.4 \pm 0.6) \times 10^3$ | |

buffer, with $SO_2$, with thiosulfate, or with other unusual conditions or poor data quality. The results are as follows:

$$C_1 = (3.7 \pm 0.63) \times 10^3 \text{ cm}^2 \text{ mol}^{-1/2} \text{ s}^{-1/2}$$

$$C_2 = (0.093 \pm 0.022) \times 10^3 \text{ cm}^2 \text{ mol}^{-1/2} \text{ s}^{-1/2}$$

Tables 1 and 2 give the ratio of the predicted and measured rates of sulfite oxidation. The overall fit of the data is reasonably good, with an average absolute deviation of 35% from the experimental oxidation rates. Therefore, the rate of sulfite oxidation is proven to increase with increasing $NO_2$ absorption rate as well as increasing sulfite and $O_2$ concentration. The data that show the largest deviation from the model occurred with no buffer and relatively high $NO_2$ in the gas phase. Under these conditions, the depletion of $SO_3^{2-}$ at the interface due to oxidation was extreme, and the interfacial solution pH could be significantly below the model prediction, which in turn would lead to inaccurate prediction of $[SO_3^{2-}]_i$ and the rate of sulfite oxidation by the model.

The results of a series of experiments with gas-phase $SO_2$ that were not used in the regression are also given in Tables 1 and 2. Previously, we have shown the effect of $SO_2$ on $NO_2$ absorption into sulfite solutions. The absorption of $SO_2$ into sulfite solutions leads to an increase in the interfacial S(IV) concentration, which, in the presence of a buffer, results in a higher rate of $NO_2$ absorption as well as sulfite oxidation. On the other hand, when no buffer is present, $SO_2$ absorption leads to a decrease in interfacial solution pH, which in turn reduces the concentration of $SO_3^{2-}$ at the interface, resulting in slower rates of $NO_2$ absorption and sulfite oxidation.

Figure 2 gives rates of sulfite oxidation calculated from eq 16. The rate of sulfite oxidation increases with increasing sulfite concentration and $NO_2$ absorption. With 15% oxygen, the rate of sulfite oxidation varies from 7 to 300 times the rate of $NO_2$ absorption. Because the experimental data points include ranges of S(IV), they do not fall on the calculated lines at exact values of S(IV).

Table 4 includes other experiments with added chloride, $Fe^{2+}$, and EDTA to determine their effects on sulfite oxidation in the presence of $NO_2$. These experimental results are compared to the predictions of eq 16. Chloride at 600 mM reduces the rate of $NO_2$ absorption, but increases the rate of oxidation almost a factor of 2. Clarke and Radojevic (*26*) found that sulfite oxidation in the absence of $NO_2$ was enhanced with $>10^{-3}$ M chloride. The catalytic effect of chloride could result from reducing the concentration of sulfate radical, which could otherwise participate in a termination reaction:

$$SO_4^{\bullet-} + Cl^- \rightarrow SO_4^{2-} + Cl^{\bullet}$$

$$Cl^{\bullet} + Cl^- \rightarrow Cl_2^{\bullet-}$$

$$Cl_2^{\bullet-} + SO_3^{2-} \rightarrow 2Cl^- + SO_3^{\bullet-}$$

**TABLE 4. Selected Continuous Experiments with Other Anions, Cations, and Metals, 55 °C, 15% $O_2$, 0.1 M Succinate, 0.25−0.3 M $Na_2SO_4$**

| pH | $[S(IV)]_b$ (mM) | $[SO_3^{2-}]_i$ (mM) | $P_{NO_2,i} \times 10^6$ (atm) | $R_{g,exp} \times 10^6$ (mol/(cm² s atm)) | $R_{g,mod}/R_{g,exp}$ | $N_{ox} \times 10^8$ (mol/(cm² s)) | $N_{ox,mod}/N_{ox,exp}$ | additive (mM) |
|---|---|---|---|---|---|---|---|---|
| 5.0 | 38.7 | 2.0 | 74 | 3.8 | 1.58 | 1.60 | 0.48 | 600 NaCl |
| 5.1 | 37.8 | 1.57 | 82 | 2.1 | 1.11 | 0.40 | 0.88 | 500 $MgSO_4$[a] |
| 5.0 | 7.12 | 2.21 | 87 | 7.1 | 1.66 | 0.41 | 0.48 | 300 $CaCl_2$ |
| 5.0 | 6.0 | 0.22 | 79 | 1.6 | 1.70 | 0.51 | 0.55 | 300 $MgCl_2$ |
| 5.65 | 6.43 | 0.96 | 64 | 3.2 | 1.31 | 0.71 | 0.74 | 0.02 $Fe^{2+}$ |
| 5.61 | 7.15 | 1.05 | 0 | 0 | 1.15 | 0.30 | 0.67 | 0.026 $Fe^{2+}$ |
| 5.65 | 6.75 | 1.03 | 49.2 | 5.0 | 0.94 | 0.65 | 1.08 | 0.02 EDTA |
| 5.52 | 7.16 | 0.91 | 0 | 0 | 0.78 | 0.13 | 1.21 | 0.02 EDTA |
| 5.57 | 6.26 | 0.82 | 15.65 | 1.93 | 1.25 | 0.37 | 0.82 | 0.017 $Fe^{2+}$ |

[a] 0.3 M succinate.

**TABLE 5. Summary of Batch Results, 200−1000 ppm $NO_2$**

| reagent (M) | pH | $O_2$ (%) | $R_g \times 10^6$ (mol/(cm² s atm)) | $k_2 \times 10^{-5}$ ($M^{-1}$ $s^{-1}$) | T (°C) |
|---|---|---|---|---|---|
| 0.085[a] $Na_2SO_3$ | 9.6 | 0 | 39.5 | 6.3 | 25 |
| 0.085[a] $Na_2SO_3$ | 9.6 | 0 | 41.3 | 18.7 | 55 |
| 0.45[a] $Na_2SO_3$ | 10.1 | 0 | 57.7 | 0.94 | 10 |
| 0.45[a] $Na_2SO_3$ | 10.1 | 0 | 73.9 | 1.9 | 15 |
| 0.45[a] $Na_2SO_3$ | 10.1 | 0 | 49.5 | 2.0 | 25 |
| 0.085[a] $Na_2SO_3$ | 9.6 | 15 | 18.2 | 1.1[b] | 25 |
| 0.09[a] $NaHSO_3$ | 4.2 | 0 | 3.8 | 0.083 | 25 |
| 0.1 $Na_2S_2O_3$ | 8.7 | 0 | 4.7 | 0.079 | 25 |
| 0.1 $Na_2SO_3$ and 0.1 $Na_2S_2O_3$ | 9.6 | 0 | 39.0 | 6.0 | 25 |
| 0.1 $Na_2SO_3$ and 0.5 $Na_2S_2O_3$ | 9.2 | 0 | 35.6 | 5.1 | 25 |
| 0.085 $Na_2S$ and 0.1 NaOH | 12.3 | 0 | 34.6 | 4.7 | 25 |
| 0.085 $Na_2S$ and 0.1 NaOH | 12.3 | 15 | 16.8 | 2.5 | 25 |
| 0.1 $Na_2S$, 0.1 NaOH, and 0.5 $Na_2S_2O_3$ | 12.7 | 15 | 32.8 | 9.4 | 25 |
| pure $H_2O$ | | 0 | 3.1 | 271[c] | 25 |

[a] These concentrations were estimated empirically by taking into account the oxidation of $SO_3^{2-}$ prior to each experiment. [b] $k_2$ was calculated using an interfacial $[SO_3^{2-}]$, estimated by BMREP. [c] $k_{2,H_2O}$ (see eq 6).

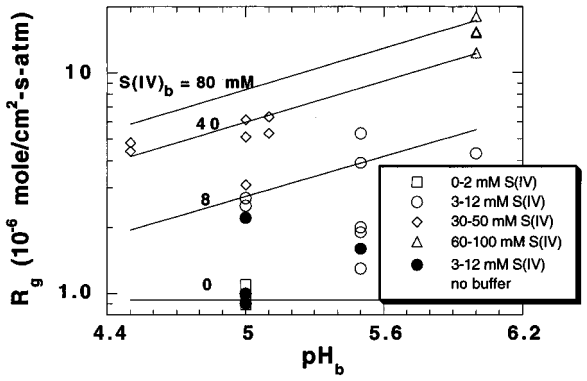


**FIGURE 1. Predicted and measured rates of $NO_2$ absorption. Most contain succinate buffer, 55 °C, 15% $O_2$. $Y_{NO_2,i}$ (ppm): calculated = 100, measured = 15−290. Lines represent model prediction by eq 7.**

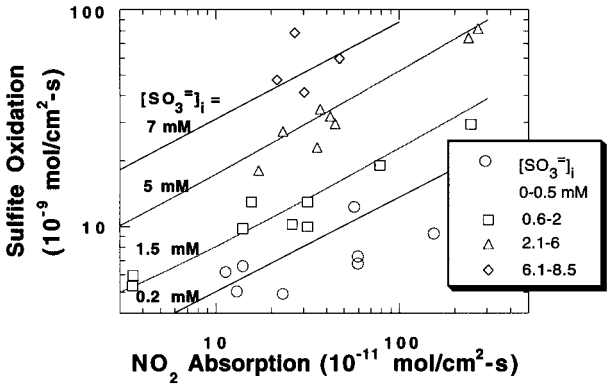


**FIGURE 2. Model prediction of sulfite oxidation, pH = 5−7, 15% $O_2$, $Y_{NO_2,i}$ = 30−350 ppm.**

The results with added $Fe^{2+}$ and EDTA show that $Fe^{2+}$ is an insignificant catalyst of sulfite oxidation in the presence of $NO_2$, although it can have a significant effect at lower rates of oxidation in the absence of $NO_2$. EDTA (0.02 mM) was added in several experiments to eliminate the effect of $Fe^{2+}$ impurities (typically 0.005 mM in 0.3 M $Na_2SO_4$ solutions).

**Effect of Thiosulfate on Sulfite Oxidation.** In previous sections, we have shown the effect of thiosulfate on $NO_2$ absorption into sulfite solutions. Thiosulfate, as a free radical scavenger, is expected to play a more significant role in sulfite oxidation by providing an alternative route for the termination of a free radical reaction mechanism.

The free radical mechanism is initiated by the reaction between $SO_3^{2-}$ and $NO_2$ (reaction 1), and the rate of initiation is given by eq 1, with $k_{2,SO_3^{2-}} = 11.2 \times 10^5$ $M^{-1}$ $s^{-1}$ at 55 °C.

The termination step of the mechanism is the reaction between $S_2O_3^{2-}$ and a free radical $R^\bullet$ (eq 11), and the rate of termination is

$$r_t = k_t[S_2O_3^{2-}][R^\bullet] \tag{17}$$

Assuming the rate of initiation equals to the rate of termination, the steady-state concentration of $R^\bullet$ is

$$[R^\bullet] = \frac{k_{2,SO_3^{2-}}}{k_t}\frac{[NO_2][SO_3^{2-}]}{[S_2O_3^{2-}]} \tag{18}$$

The rate of oxidation is the rate of reaction between $R^\bullet$ and

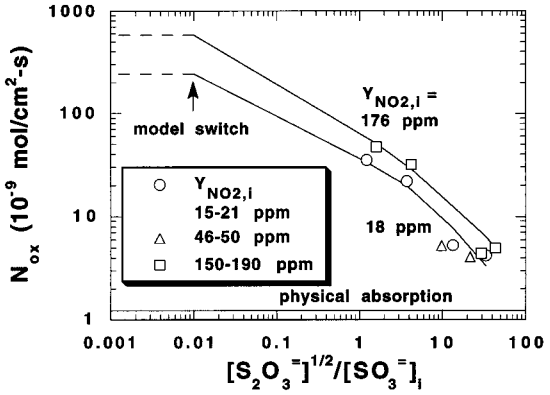


**FIGURE 3. Model prediction of sulfite oxidation in the presence of thiosulfate, pH = 5.5 and 7.5, $[SO_3^{2-}]_i$ = 7−90 mM, 55 °C, 15% $O_2$.**

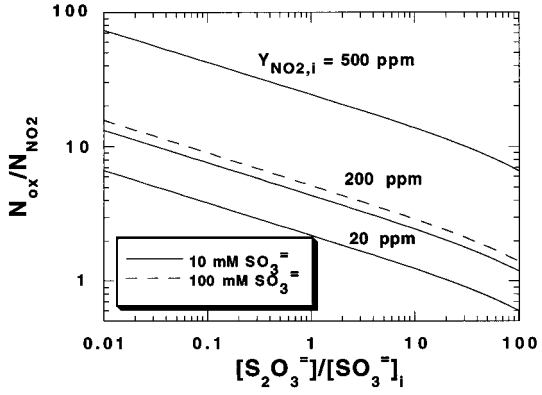


**FIGURE 4. Calculated effect of $NO_2$ and $SO_3^{2-}$ concentration on sulfite oxidation with $S_2O_3^{2-}$, pH > 7.5, 15% $O_2$, 55 °C.**

$SO_3^{2-}$:

$$r_{ox} = k_{ox}[R^{\bullet}][SO_3^{2-}] \quad (19)$$

Substituting the expression for [R•] from eq 18 into eq 19, we have

$$r_{ox} = \frac{k_{ox}k_{2,SO_3^{2-}}}{k_t}\frac{[SO_3^{2-}]^2[NO_2]}{[S_2O_3^{2-}]} \quad (20)$$

The differential mass balance is

$$-D_{O_2}\frac{d^2[O_2]}{dx^2} = r_{ox} \quad (21)$$

To simplify the calculation, $r_{ox}$ was assumed to be constant over the entire film thickness $\delta$. Equation 21 was integrated over the entire thickness of $\delta$, with the following boundary conditions:

$$@\ x = 0,\ [O_2] = [O_2]_i \text{ and } O_2 \text{ flux} = N_{ox}$$

$$@\ x = \delta,\ [O_2] = 0$$

Finally we have

$$N_{ox} = \sqrt{2D_{O_2}[O_2]_1\frac{k_{ox}k_{2,SO_3^{2-}}}{k_t}\frac{[SO_3^{2-}]_i^2[NO_2]_i}{[S_2O_3^{2-}]}} \quad (22)$$

where $D_{O_2}$ is the diffusivity of $O_2$, with a value of $4.79 \times 10^{-5}$ cm$^2$ s$^{-1}$ at 55 °C, and $N_{ox}$ is the measured rate of sulfite oxidation. A set of 10 experiments from Table 2 with varying concentrations of $[SO_3^{2-}]_i$, $[NO_2]_i$, and $[S_2O_3^{2-}]$ were used to regress the ratio of $k_{ox}$ to $k_t$. At 55 °C, only experiments with thiosulfate at normal conditions were included. The regressed ratio is

$$\frac{k_{ox}}{k_t} = 3.43$$

Owens (*23*) reported a value of 4 for the above ratio at 50 °C.

Figure 3 gives the calculated rate of sulfite oxidation as a function of thiosulfate. The rate of sulfite oxidation decreases with increasing ratio of the square root of $[S_2O_3^{2-}]$ to $[SO_3^{2-}]_i$ but increases with $Y_{NO_2,i}$. An order of magnitude increase in the concentration of interfacial $NO_2$ leads to a factor of 3 increase in $N_{ox}$, consistent with the expression in eq 16. Furthermore, even with $([S_2O_3^{2-}]^{1/2}/[SO_3^{2-}]_i$ of 40, the rate of sulfite oxidation was still 3−4 times higher than that of physical absorption, indicating that sulfite oxidation is unavoidable with $NO_2$ absorption, even with the addition of thiosulfate. Noticeable deviation from the model is observed in two runs with 46−50 ppm $NO_{2,i}$. This is due to the fact that the solution pH for these two runs was around 5.5. At this pH, the oxidation of $HSO_3^-$ started to become significant (*23*). All other runs in Figure 3 had pH > 7.5.

Figure 3 also shows the continuity between our model of sulfite oxidation without thiosulfate (eq 16) and the model of sulfite oxidation in the presence of thiosulfate (eq 22). When $([S_2O_3^{2-}])^{1/2}/[SO_3^{2-}]_i$ is greater than 0.01, the rate of sulfite oxidation can be predicted from eq 22. When $([S_2O_3^{2-}])^{1/2}/[SO_3^{2-}]_i$ is less than 0.01, eq 16 should be used to predict the rate of sulfite oxidation. The curves representing the two models intersected at $([S_2O_3^{2-}])^{1/2}/[SO_3^{2-}]_i$ = 0.01 for both $NO_2$ concentrations shown in Figure 3.

It has also become possible to estimate the number of moles of S(IV) oxidized for every mole of $NO_2$ absorbed in the presence of thiosulfate. The ratio of moles S(IV) oxidized to moles $NO_2$ absorbed can be expressed as the ratio of the rate of sulfite oxidation to the rate of $NO_2$ absorption, which is

$$\frac{N_{ox}}{N_{NO_2}} = \frac{\sqrt{2D_{O_2}[O_2]_i\frac{k_{ox}k_{2,SO_3^{2-}}}{k_t}\frac{[SO_3^{2-}]_i^2[NO_2]_i}{[S_2O_3^{2-}]}}}{\frac{P_{NO_{2,i}}}{H_{NO_2}}\sqrt{D_{NO_2}(k_{2,SO_3^{2-}}[SO_3^{2-}]_i + k_{2,S_2O_3^{2-}}[S_2O_3^{2-}]_i)}} \quad (23)$$

Figure 4 gives the above ratio as a function of $([S_2O_3^{2-}])^{1/2}/[SO_3^{2-}]_i$ at several interfacial $NO_2$ concentrations. The ratio of oxidation to $NO_2$ absorption decreases with increasing $([S_2O_3^{2-}])^{1/2}/[SO_3^{2-}]_i$ and decreasing $NO_2$ concentration, and it is not a strong function of $[SO_3^{2-}]_i$.

**Results of Batch Experiments.** A series of experiments were performed by operating the stirred-cell contactor in batch mode. The results of these experiments are summarized in Table 4. The second-order reaction rate constant ($k_2$) is given for the reaction between $NO_2$ and the primary reagent. Each of the experiments included a series of measurements with 200−1000 ppm $NO_2$. The absorbent concentrations given in Table 4 were not determined by solution analysis. They are either the nominal concentrations as prepared gravimetrically from reagent chemicals or the nominal concentration corrected for expected sulfite oxidation. Most of these experiments were performed at 25 °C and without $O_2$, so they are not directly comparable to the continuous experiments at 55 °C and in the presence of $O_2$.

Figure 5 gives $NO_2$ absorption as a function of $P_{NO_2,i}$ with 0.085−0.1 M reagents. The fastest rate of $NO_2$ absorption occurred in solutions of sulfite, indicating that it is the most effective reagent. On the other hand, $NO_2$ absorption in

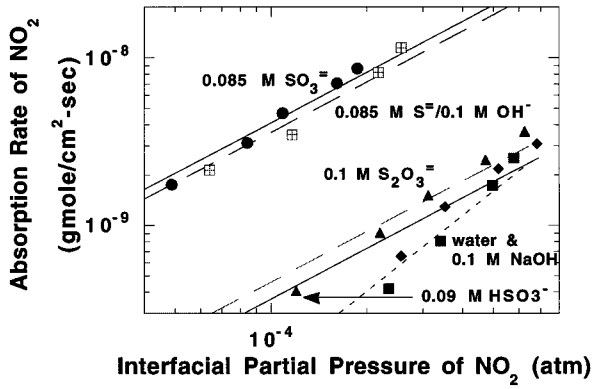


**FIGURE 5. $NO_2$ absorption batch experiments, 25 °C, no $O_2$.**

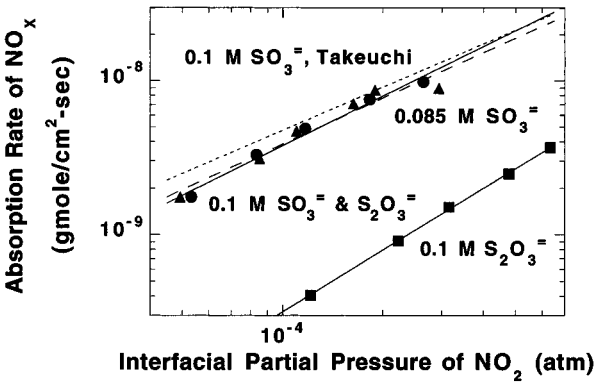


**FIGURE 6. $NO_2$ absorption into sulfite, thiosulfate, and mixture at 25 °C.**

thiosulfate or bisulfite solution is only slightly greater than in pure water. This trend was also observed by Takeuchi et al. (*5*).

Several of the batch experiments were intended to clarify the effect of $O_2$ on $NO_2$ absorption. The addition of 15% $O_2$ to the gas stream reduces $NO_2$ absorption in 0.1 M $Na_2SO_3$ solution by a factor of 2. However, the addition of $Na_2S_2O_3$ eliminates this effect, as shown in Figure 6. This is the same observation we have made with our continuous experiments. Takeuchi et al. (*22*) also reduced the oxidation effect with other inhibitors.

**Industrial Implications.** With the reaction rate constants between sulfite and $NO_2$, we can predict the $NO_2$ removal in a typical limestone slurry scrubber by:

$$\frac{1}{\ln\dfrac{Y_{NO_{2,in}}}{Y_{NO_{2,out}}}} = \frac{1}{N_g} + \frac{GH_{NO_2}}{A\sqrt{k_1 D_{NO_2}}} \qquad (24)$$

In eq 24, $Y_{NO_2}$ is the mole fraction of $NO_2$, $A$ is the gas−liquid contact area, and $G$ is the gas flow rate. $N_g$, the number of gas film transfer units, was taken to be 6.9, typical of limestone slurry scrubbing (*27*). The ratio $A/G$ was taken to be $2 \times 10^5$ atm $cm^{-2}$ $s^{-1}$ $mol^{-1}$. The effective first-order rate constant is given by

$$k_1 = k_{2,SO_3^{2-}}[SO_3^{2-}]_i + k_{2,HSO_3^-}[HSO_3^-] + \frac{2k_{2,H_2O}P_{NO_{2,i}}}{3H_{NO_2}} \qquad (25)$$

Figure 7 plots the fractional penetration of $NO_2$ as a function of interfacial S(IV) concentration in a typical scrubber. With typical conditions for limestone slurry, 10 mM total dissolved S(IV) and pH 4−5, the estimated $NO_2$ removal is less than 50%. Therefore, an acceptable level of

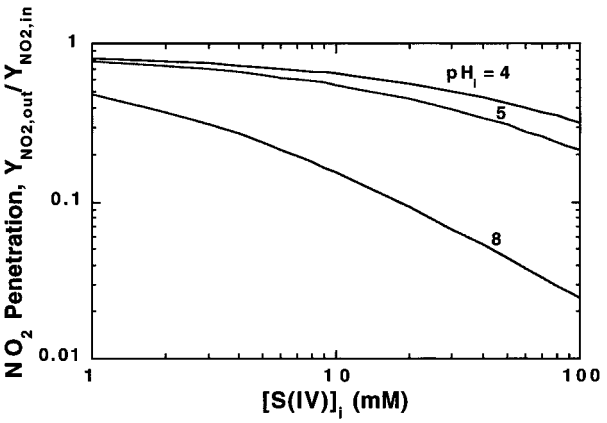


**FIGURE 7. $NO_2$ removal in a typical limestone slurry scrubber. $N_g = 6.9$, $k_g = 3.4 \times 10^{-5}$ mol $cm^{-2}$ $s^{-1}$ $atm^{-1}$. Difference between solid and dotted line reflects the effect of $NO_2$ concentration on fraction $NO_2$ removal.**

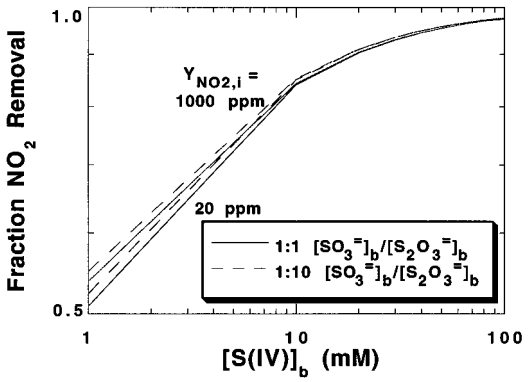


**FIGURE 8. $NO_2$ removal in an aqueous $Na_2SO_3$ scrubber. $N_g = 6.9$, $k_g = 3.4 \times 10^{-5}$ mol $cm^{-2}$ $s^{-1}$ $atm^{-1}$, pH > 7.5, 55 °C, 15% $O_2$.**

$NO_2$ removal by a conventional limestone slurry scrubber is not probable. Marginally acceptable performance might be possible in a forced oxidation system promoted by organic acids and by magnesium or sodium sulfate and controlled at the maximum level of dissolved sulfite.

However, our study also shows that $Na_2SO_3$ scrubbing, with the addition of $Na_2S_2O_3$ at high pH, is capable of achieving 95% $NO_2$ removal as shown in Figure 8. At pH 7.5, 80 mM or more total dissolved sulfite and at least a molar ratio of 1:1 thiosulfate sulfite are necessary for 95% removal of $NO_2$. Increasing the ratio of thiosulfate to sulfite does not lead to significant enhancement in $NO_2$ removal, but it would reduce the rate of sulfite oxidation and minimize the consumption of $SO_3^{2-}$.

Our study of sulfite oxidation also shows that it may be feasible to reduce the liquid depth in the hold tank in limestone slurry scrubbing by the addition of $NO_2$. $NO_2$ can be mixed with air and sparged into the hold tank, and oxidation in the hold tank will increase, resulting in considerable reduction of required liquid depth in the tank. By assuming a liquid depth of 30 ft is required to absorb 50% of the oxygen in the inlet air via physical absorption, a calculation was performed by integrating the $NO_2$-enhanced rate of oxidation over the new depth of liquid required to achieve the same level of oxygen absorption.

The calculated results in Figure 9 show that a significant reduction in hold tank liquid depth can be achieved by injecting 1000 ppm $NO_2$ at the bottom of the hold tank. This represents 1 mol of $NO_2$ injected for every 100 mol of $O_2$ absorbed. This ratio of $NO_2$:$O_2$ absorbed was necessary because the $NO_2$ was rapidly consumed by reaction with sulfite and thus was only able to initiate oxidation in a small

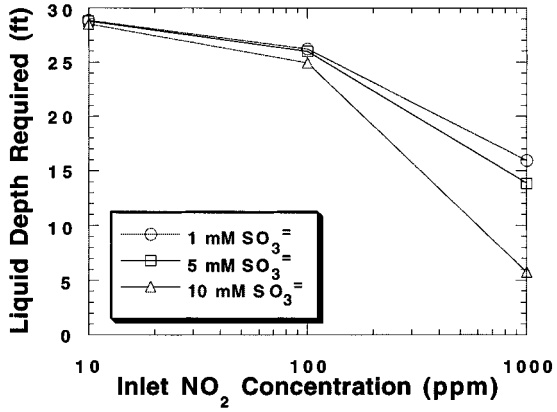


**FIGURE 9. Reduction of hold tank liquid depth reduction by $NO_2$ injection. $Y_{O_2,in} = 0.2$, $Y_{O_2,out} = 0.1$. $A'/G = 1.9 \times 10^4$ cm $s^{-1}$ $mol^{-1}$. $NO_2$ injection at bottom of tank, 55 °C.**

segment of the liquid. An alternative method of $NO_2$ addition would be to inject smaller amounts of $NO_2$ at several different liquid depths. Since each injection of $NO_2$ would initiate sulfite oxidation over a small liquid depth, a lower concentration of $NO_2$ might be used.

## Acknowledgments

This study has been supported by the Environmental Solutions Program of the University of Texas at Austin and by the United States Environmental Protection Agency.

## Nomenclature

| | |
|---|---|
| $A$ | interfacial area, $cm^2$ |
| $C_1$, $C_2$, $C_3$ | regressed constants in sulfite oxidation model |
| $D_{NO_2}$ | diffusion coefficient of $NO_2$, $cm^2/s$ |
| $D_{O_2}$ | diffusion coefficient of $O_2$, $cm^2/s$ |
| $G$ | gas flow rate, L/min |
| $H_{NO_2}$ | Henry's constant of $NO_2$, $cm^3$ $atm^{-1}$ $mol^{-1}$ |
| $[HSO_3^-]_b$, $[HSO_3^-]_i$ | bulk and interfacial concentration of $HSO_3^-$, M |
| $k_{2,H_2O}$ | reaction rate constant for $NO_2$ and water, $M^{-1}$ $s^{-1}$ |
| $k_{2,HSO_3^-}$ | reaction rate constant for $NO_2$ and bisulfite, $M^{-1}$ $s^{-1}$ |
| $k_{2,S_2O_3^{2-}}$ | reaction rate constant for $NO_2$ and thiosulfate, $M^{-1}$ $s^{-1}$ |
| $k_{2,SO_3^{2-}}$, $k_{ini}$ | reaction rate constant for $NO_2$ and sulfite, $M^{-1}$ $s^{-1}$ |
| $k_g$ | gas-phase mass transfer coefficient, mol $cm^{-2}$ $s^{-1}$ $atm^{-1}$ |
| $k_l^\circ$ | liquid-phase mass transfer coefficient, cm $s^{-1}$ |
| $k_{ox}$ | reaction rate constant for oxidation reaction, $M^{-1}$ $s^{-1}$ |
| $k_t$ | reaction rate constant for termination step, $M^{-1}$ $s^{-1}$ |
| $K_g$ | overall gas-phase mass transfer coefficient, mol $cm^{-2}$ $s^{-1}$ $atm^{-1}$ |
| $N_g$ | number of gas film transfer units |
| $N_{NO_2}$ | flux of $NO_2$, mol $cm^{-2}$ $s^{-1}$ |
| $N_{ox}$ | rate of sulfite oxidation, mol $cm^{-2}$ $s^{-1}$ |
| $[NO_2]_i$ | interfacial concentration of $NO_2$, M |
| $N_{SO_2}$ | rate of $SO_2$ absorption, mol $cm^{-2}$ $s^{-1}$ |
| $[O_2]_i$ | interfacial $O_2$ concentration, M |
| $P_{NO_2,b}$, $P_{NO_2,i}$ | bulk and interfacial partial pressure of $NO_2$, atm |
| $r$ | rate of reaction, mol $L^{-1}$ $s^{-1}$ |
| $R_g$ | normalized rate of $NO_2$ absorption, mol $cm^{-2}$ $s^{-1}$ $atm^{-1}$ |
| $[SO_3^{2-}]_b$, $[SO_3^{2-}]_i$ | bulk and interfacial concentration of $SO_3^{2-}$, M |
| $[SO_5^{\bullet-}]$ | concentration of $SO_5^{\bullet-}$ radical, M |
| $[S(IV)]_o$, $[S(IV)]_f$ | initial and final concentration of S(IV), M |
| $[S(IV)]_{tit}$ | concentration of S(IV) in solution added to contactor, M |
| $\Delta t$ | time interval, s |
| $V$ | solution volume, L |
| $V_{tit}$ | volume of solution added to contactor, mL |
| $Y_{NO_2}$ | $NO_2$ mole fraction |
| $Y_{NO_2,b}$, $Y_{NO_2,i}$ | bulk and interfacial concentration of $NO_2$, ppm |
| $\delta$ | film thickness, cm |

## Literature Cited

(1) Lyon, R. K.; Cole, J. A.; Kramlich, J. C.; Chen, S. L. *Combust. Flame* **1991**, *81*, 30.
(2) Izumi, J.; Murakami, N. U.S. Patent 4,350, 669, September 21, 1982.
(3) Borders, R. A.; Birks, J. W. *J. Phys. Chem.* **1982**, *86*, 3295.
(4) Baveja, K. K.; Rao, D. S.; Sarkar, M. K. *J. Chem. Eng. Jpn.* **1979**, *12*, 322−325.
(5) Takeuchi, H.; Ando, M.; Kizawa, N. *Ind. Eng. Chem., Process Des. Dev.* **1977**, *16*, 303.
(6) Takeuchi, H.; Yamanaka, Y. *Ind. Eng. Chem., Process Des. Dev.* **1978**, *17*, 389.
(7) Kameoka, Y.; Pigford, R. L. *Ind. Eng. Chem., Fundam.* **1977**, *16*, 163.
(8) Littlejohn, D.; Wang, Y.; Chang, S.-G. *Environ. Sci. Technol.* **1993**, *27*, 2161.
(9) Shen, C.; Rochelle, G. T. Nitrogen Dioxide Absorption and Sulfide Oxidation in Aqueous Sulfide. *J. Air Waste Manage. Assoc.* In press.
(10) Shen, C. Nitrogen Dioxide Absorption in Aqueous Sodium Sulfite. Ph.D. Dissertation, The University of Texas at Austin, May 1997.
(11) McGuire, L. M. Sulfur Dioxide Absorption Experiments in Calcium Hydroxide Slurries. M.S. Thesis, University of Texas at Austin, 1990.
(12) Tseng, C. H. P. Calcium Sulfite Hemihydrate Dissolution and Crystallization. Ph.D. Dissertation, University of Texas at Austin, 1984.
(13) Thorn, P. R., Jr. Diethlenetriamine Solutions for Stack Gas Desulfurization by Absorption/Stripping. M.S. Thesis, University of Texas at Austin, 1981.
(14) Nash, T. *Atmos. Environ.* **1979**, *13*, 1149.
(15) Danckwerts, P. V. Absorption into Agitated Liquids. In *Gas−Liquid Reactions*; McGraw-Hill: New York, 1970.
(16) Glasscock, D. A.; Rochelle, G. T. *AIChE J.* **1993**, *39*, 1389.
(17) Wilke, C. R.; Chang, P. *AIChE J.* **1955**, *1*, 261.
(18) Andrew, S. P. S.; Hanson, D. *AIChE J.* **1965**, *11*, 105.
(19) Oblath, S. B.; Markowitz, S. S.; Novakov, T.; Chang, S. G. *J. Phys. Chem.* **1982**, *86*, 4853.
(20) Oblath, S. B.; Markowitz, S. S.; Novakov, T.; Chang, S. G. *J. Phys. Chem.* **1981**, 85, 1017.
(21) Huie, R. E.; Neta, P. *J. Phys. Chem.* **1984**, *88*, 5665.
(22) Takeuchi, H.; Takahashi, K.; Kizawa, N. *Ind. Eng. Chem., Process Des. Dev.* **1977**, *16*, 486.

(23) Owens, D. R. Sulfite Oxidation Inhibited by Thiosulfate. M.S. Thesis, University of Texas at Austin, 1984.

(24) Epstein, M. *EPA Alkali Scrubbing Test Facility: Summary of Testing Through October 1974*. EPA-650/2-75-047; NTIS PB-244 901; U.S. Government Printing Office: Washington, DC, 1975.

(25) Clifton, C. L.; Altstein, N.; Huie, R. E. *Environ. Sci. Technol.* **1988**, *22*, 5586−589.

(26) Clarke, A. G.; Radojevic, M. *Atmos. Environ.* **1983**, *17*, 617.

(27) Agarwal, R. S. Limestone Slurry Scrubbing-Modeling and Parameter Estimation. Ph.D. Dissertation, University of Texas at Austin, 1995.

*Received for review May 27, 1997. Revised manuscript received April 14, 1998. Accepted April 20, 1998.*

ES970466Q